

## Cationic diffusion in $\text{La}_{2/3}\text{Ca}_{1/3}\text{MnO}_3$ thin films grown on $\text{LaAlO}_3$ (001) substrates

S. Estradé,<sup>a)</sup> J. Arbiol, and F. Peiró

EME/CeRMAE/IN<sup>2</sup>UB, Departament d'Electrònica, Universitat de Barcelona, c/Marti Franques 1, 08028 Barcelona, Spain

Ll. Abad, V. Laukhin, Ll. Balcells, and B. Martínez

Institut de Ciència de Materials de Barcelona-CSIC, 08193 Bellaterra, Spain

(Received 3 July 2007; accepted 26 September 2007; published online 19 December 2007)

Microstructural features of  $\text{La}_{2/3}\text{Ca}_{1/3}\text{MnO}_3$  layers of various thicknesses grown on top of (001)  $\text{LaAlO}_3$  substrates are studied by using transmission electron microscopy and electron energy loss spectroscopy. Films are of high microstructural quality but exhibit some structural relaxation and mosaicity both when increasing thickness or after annealing processes. The existence of a cationic segregation process of La atoms toward free surface has been detected, as well as a Mn oxidation state variation through layer thickness. La diffusion would lead to a Mn valence change and, in turn, to reduced magnetization. © 2007 American Institute of Physics. [DOI: 10.1063/1.2799740]

Due to their strong magnetoresistive response and their half metallic character manganese perovskites are considered as one of the ideal candidates for the implementation of magnetoelectronic devices. In particular, strong interest has been concentrated on the fabrication of magnetic tunnel junctions (MTJs) because of their potential application for the implementation of magnetic memory devices.<sup>1,2</sup> Nevertheless, they have failed to live up to initial expectations since the response of manganite-based MTJs yields Curie point  $T_C$  values clearly below those corresponding to bulk material.<sup>3-5</sup>

The origin of this strong degradation of magnetotransport properties with temperature is not well understood yet. Structural strain due to the substrate/film mismatching has been suggested as a possible cause of this degradation; therefore, different substrates as  $\text{LaAlO}_3$  (LAO) or  $\text{SrTiO}_3$  (STO) have been investigated in order to clarify this point.<sup>5,6</sup> Whereas  $\text{La}_{2/3}\text{Ca}_{1/3}\text{MnO}_3$  (LCMO) on STO grows under tensile, moderate strain ( $\approx +1.2\%$ ) allowing us to get a defect-free epitaxy, the LCMO on LAO, grows under compressive, greater strain ( $\approx -1.8\%$ ) leading to a three-dimensional (3D) growth process with misfit dislocations and twins and depressed magnetic properties.<sup>5,6</sup> Nevertheless, little attention has been paid to the influence of other physical phenomena besides microstructural defects in order to explain the depressed magnetic properties observed on LCMO/LAO films.

In the present work, we have performed a careful study of the microstructure of LCMO/LAO films prepared using rf sputtering as a function of thickness in as-grown (AG) and annealed samples. Samples have been characterized by high resolution transmission electron microscopy (HRTEM) and electron energy loss spectroscopy (EELS), paying special attention to the determination of the quality of the LCMO/LAO interfaces, and to the compositional homogeneity. The existence of a cationic segregation process of La atoms toward the surface of the films has been identified and correlated with the degradation of the magnetic properties.

LCMO layers were grown by rf sputtering on top of (001) LAO substrates with nominal thicknesses ranging from 14 to 93 nm at a deposition temperature of 800 °C, a depo-

sition pressure of 330 mtorr, and an  $\text{O}_2/\text{Ar}$  pressure ratio of 1/4; afterwards, they were submitted to an *in situ* annealing process in an  $\text{O}_2$  atmosphere at a pressure of 350 torr and at a temperature of 800 °C for 60 min;<sup>7</sup> every such sample was annealed at  $T_a=1000$  °C, also keeping an as-grown sample for comparison.

The samples, prepared in cross section geometry by flat polishing down to 50  $\mu\text{m}$ , followed by a dimpling down to 25  $\mu\text{m}$  and a final  $\text{Ar}^+$  bombardment at  $V=5$  kV with an incident angle of 7° using a PIPS-Gatan equipment, were observed by HRTEM in a Jeol J2010F microscope, with field emission gun, operating at 200 keV. EELS spectra were obtained with a Gatan image filter (GIF) spectrometer. Ca/La normalized relative concentration variations were obtained from EELS spectra by integrating the intensity corresponding to Ca and La peaks, getting the relative intensity for each studied point and dividing such figure by the value obtained in a reference position, which was chosen to be the one closest to the interface. Mn  $L_3$  EELS peak edge and Mn  $L_3/\text{Mn } L_2$  peak intensity ratio were determined using home-made program "MANGANITAS." This is a MATLAB routine that reads the EEL spectrum file, locates O  $K$  peak onset and recalibrates energy axis using this O  $K$  peak as a reference. Then, it performs a fitting of both the background and continuum signal and subtracts them. Finally, it estimates Mn  $L_3$  peak onset, fits Gaussian curves to both Mn  $L_3$  and Mn  $L_2$  peaks, and integrates the Gaussian curves, using integration ranges that have been chosen by quantification of LCMO reference bulk samples with controlled stoichiometry. Magnetic properties were measured by using a commercial superconducting quantum interference device magnetometer from Quantum Design.

HRTEM images of AG (a) and annealed (b) 14 nm thick samples along the [100] zone axis are shown in Fig. 1. Abrupt, flat, and homogeneous interfaces between LCMO film and LAO substrate, and LCMO free surfaces were found in the thinnest AG samples [Fig. 1(a)]. Nevertheless, interfaces between LCMO film and LAO substrate, and LCMO free surfaces, were found to get slightly rougher as layer thickness increases and with the annealing treatment. The layers were determined to be homogeneous and defect-free at

<sup>a)</sup>Electronic mail: sestrade@el.ub.es

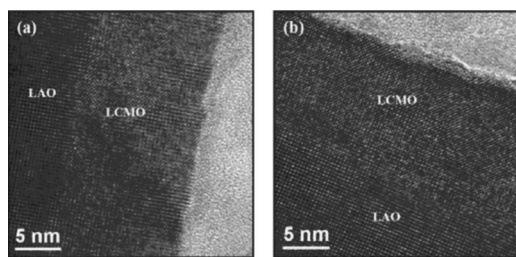


FIG. 1. High resolution images of as grown (a) and annealed (b) 14 nm thick samples along the [100] zone axis.

least in the studied region, with mosaicity increasing again with thickness and after annealing treatments.

The nominal epitaxial relationship LCMO (001) [100]||LAO(001)[100] was found, by fast Fourier transform (FFT) of high resolution images of layer and substrate, for all studied samples. High resolution images were also studied by Gaussian fitting of intensities corresponding to atomic columns, as to locate their relative positions with high precision;<sup>8,9</sup> this method was used to determine lattice parameters instead of FFT. Lattice parameters as determined by transmission electron microscopy (TEM) are in good agreement with those found by x-ray diffraction (XRD) (Table I); out-of-plane  $c$  parameter decreases while in-plane  $a$  parameter increases, after annealing processes and/or when increasing film thickness, approaching bulk values as in-plane stress gradually relaxes.

The compositional profiles along sample thickness were analyzed by EELS in cross sections of the different samples. Initially, general spectra (between 325 and 870 eV) were acquired along the direction perpendicular to the interface going from the substrate/film interface toward the free surface of the layer. The evolution of the Ca/La ratios in LCMO layers were estimated from the general spectra and the corresponding results are displayed in Fig. 2. In all cases, a cationic segregation process leading to an increase of the La content while approaching film surface was detected, while the Ca/La variation rate slows down with annealing process and/or by increasing sample thickness.

EELS spectra in the energy loss range between 500 and 675 eV [in which the Mn  $L_{2,3}$  peaks (640 and 651 eV) and the O  $K$  peak (532 eV) can be found] were also investigated.

Once the position of the LCMO/LAO interface was fixed, a sequential acquisition of EELS spectra at different distances from the interface was carried out.

EELS spectra have been widely used to determine Mn oxidation state.<sup>10-15</sup> In our case, the measurements of peak edge and Mn  $L_3$ /Mn  $L_2$  peak intensity ratio were determined using aforementioned homemade program “MANGANTAS.” The experimental results are illustrated in Fig. 3 in comparison with the theoretical values found in literature<sup>13-15</sup> for the Mn oxidation states of 2+, 3+, and 4+. The most relevant

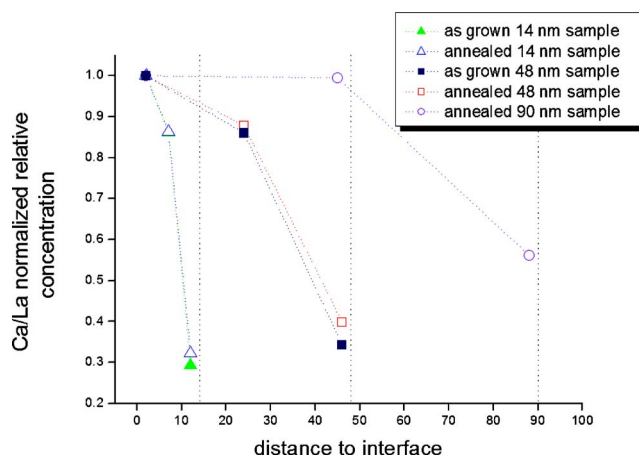


FIG. 2. (Color online) Ca/La normalized relative concentration variation for several as-grown and annealed LCMO/LAO samples having different thicknesses.

feature in Fig. 3 is a shift toward lower energies of the Mn  $L_{2,3}$  peaks as well as a variation of the intensity ratio of these two peaks as the distance from the interface is increased. According to the data corresponding to bulk reference samples, these observations imply that the Mn oxidation state would significantly change along the layer thickness. Even more, this variation of the Mn oxidation state is also compatible with the detected La diffusion toward the free surface of the films, as suggested by the observed variation of the La/Ca ratio, more pronounced for thinner and as-grown samples.

As previously mentioned LCMO on LAO, grows under compressive strain ( $\approx -1.8\%$ ) leading to an increase of the out-of-plane parameter  $c$ . This elongation of the unit cell along the  $c$  axis induces an easy magnetization axis perpendicular to the film plane. The departure of the easy magnetization axis from perpendicular to film plane to parallel to plane has been observed as structural strain relaxes by increasing film thickness or by high temperature annealing processes.<sup>16</sup> On the other hand, both saturation magnetization  $M_S$  and  $T_C$  exhibit a clear dependence on sample thickness (see Fig. 4). In this figure we also show that the high temperature annealing process substantially improves magnetic properties, and that this improvement is notoriously stronger in thinner samples. At first sight this evolution of  $T_C$  and  $M_S$  could be correlated with variations of structural strain; nevertheless, as pointed out by Biswas *et al.*,<sup>17</sup> the LCMO/LAO system exhibits a 3D growth mechanism from the early stages leading to a granular character of the films and making it very difficult to obtain a homogeneously strained film. Besides, in-plane biaxial compression, as in LCMO/LAO system, should imply an expansion of the out-of-plane parameter because of the Poisson effect leading to a flattening of the Mn–O–Mn angle, thus promoting a reduc-

TABLE I. In-plane ( $a$ ) and out-of plane ( $c$ ) lattice parameters of LCMO/LAO samples determined by TEM and XRD.

Thickness	$c$ (Å) determined by TEM		$c$ (Å) determined by XRD		$a$ (Å) determined by TEM		$a$ (Å) determined by XRD	
	As grown	Annealed	As grown	Annealed	As grown	Annealed	As grown	Annealed
14 nm	3.94	3.88	3.957	3.878	3.82	3.83	3.793	3.865
48 nm	3.91	3.85	3.920	3.868	3.82	3.88	3.793	3.857
90 nm	...	3.85	3.897	3.870	...	3.86	3.820	3.853

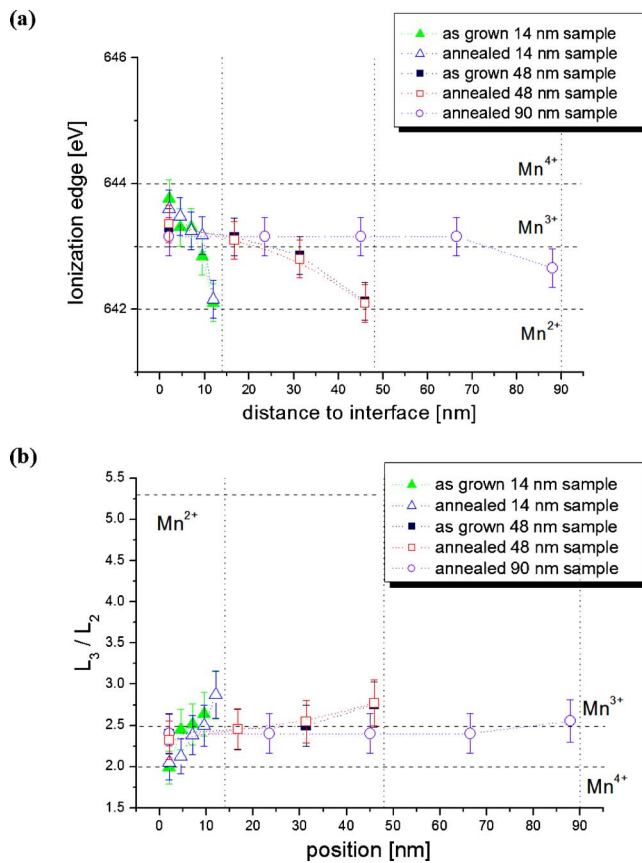


FIG. 3. (Color online) Ionization edge variation (a) and relative intensity variation (b) of the Mn  $L_3$  and Mn  $L_2$  peaks along LCMO layers.

tion of the Jahn-Teller effect and the increase of  $T_C$ ,<sup>18</sup> which is not observed in our case. Therefore, we should conclude that structural strain alone cannot account for the variations of  $T_C$  and  $M_S$ .

Interestingly enough, the observed evolution of  $T_C$  and  $M_S$  clearly correlates with the segregation process of La ions toward the surface of the films. The formation of a La floating layer during LCMO thin film growth should lead to the appearance of a La-enriched layer of a few nanometers close

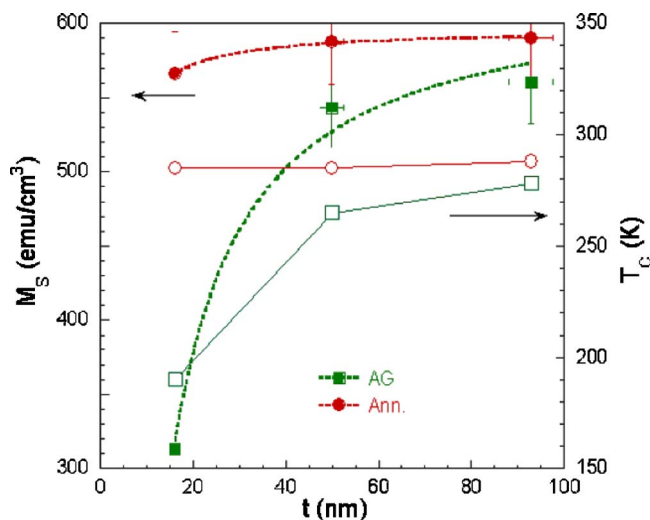


FIG. 4. (Color online) Saturation magnetisation and dependence of the transition temperature  $T_C$  as a function of sample thickness for as-grown and annealed samples.

to the free surface of the films. This layer should exhibit strongly depressed magnetic properties in agreement with the existence of a surface magnetic dead layer as detected from magnetic measurements in LCMO/LAO thin films.<sup>19</sup> Since this La-rich layer is very thin (few nanometers), its effects are negligible for thick samples but critical for thin ones. This La segregation process would, in turn, imply a departure from the nominal composition (2/3–1/3) Mn<sup>3+/4+</sup> valence balance, thus becoming an efficient mechanism for the reduction of  $T_C$  and  $M_S$ . Nevertheless, it should be mentioned that strain may be at the origin of this cationic migration since a way to accommodate structural strain in thin films could be by means of the segregation of ions with larger or smaller size. For instance, elastic strain accommodation in LCMO films grown on STO (tensile strain of about +1.2%) occurs by 2+ valence cationic migration.<sup>3</sup> In contrast, under compressive strain, as in LCMO/LAO (–1.8%), a 3+ valence cationic migration toward film surface should be expected, since La<sup>3+</sup> ionic radius (1.36 Å) is higher than Ca<sup>2+</sup> ionic radius (1.34 Å).

On the other hand, high temperature annealing processes would promote rediffusion of La ions in the whole film which would moderate the effect of the cationic migration (see Figs. 3 and 4) and substantially improve both  $T_C$  and  $M_S$ , as observed.

We acknowledge financial support from Spanish MEC (MAT2003-4161 and MAT2006-13572-C02-01), FEDER program, and Generalitat de Catalunya (2005SGR-00509).

- <sup>1</sup>J. S. Moodera and G. Mathon, *J. Magn. Magn. Mater.* **200**, 248 (1999).
- <sup>2</sup>S. S. P. Parkin, K. P. Roche, M. G. Samant, P. M. Rice, R. B. Byers, R. E. Scheuerlein, E. J. O'Sullivan, S. L. Brown, J. Bucchigano, D. W. Abraham, Y. Lu, M. Rooks, P. L. Trouilloud, R. A. Wanner, and W. J. Gallagher, *J. Appl. Phys.* **85**, 5828 (1999).
- <sup>3</sup>J. Simon, T. Walther, W. Mader, J. Klein, D. Reisinger, L. Alff, and R. Gross, *Appl. Phys. Lett.* **84**, 3882 (2004).
- <sup>4</sup>F. Pailloux, D. Imhoff, T. Sikora, A. Barthélémy, J.-L. Maurice, J.-P. Contour, C. Colliex, and A. Fert, *Phys. Rev. B* **66**, 014417 (2002).
- <sup>5</sup>E. Gommert, H. Cerva, J. Wecker, and K. Samwer, *J. Appl. Phys.* **85**, 5417 (1999).
- <sup>6</sup>K. Daoudi, T. Tsuchiya, I. Yamaguchi, T. Manabe, S. Mizuta, and T. Kumagai, *J. Appl. Phys.* **98**, 013507 (2005).
- <sup>7</sup>S. Valencia, Ll. Balcells, J. Fontcuberta, and B. Martínez, *Appl. Phys. Lett.* **82**, 4531 (2003).
- <sup>8</sup>V. Potin, E. Hahn, A. Rosenauer, D. Gerthsen, B. Kuhn, F. Scholz, A. Dussaignec, B. Damilano, and N. Grandjean, *J. Cryst. Growth* **262**, 145 (2004).
- <sup>9</sup>F. Peiró, J. C. Ferrer, A. Cornet, and J. R. Morante, *J. Vac. Sci. Technol. B* **15**, 1715 (1997).
- <sup>10</sup>T. Riedl, T. Gemming, and K. Wetzig, *Ultramicroscopy* **106**, 284 (2006).
- <sup>11</sup>Y. Q. Wang, X. F. Duan, Z. H. Wang, and B. G. Shen, *Mater. Sci. Eng., A* **333**, 80 (2002).
- <sup>12</sup>Z. L. Wang, J. Bentley, and N. D. Evans, *Micron* **31**, 355 (2000).
- <sup>13</sup>Z. L. Wang, J. S. Yin, and Y. D. Jiang, *Micron* **31**, 571 (2000).
- <sup>14</sup>H. Kurata and C. Colliex, *Phys. Rev. B* **48**, 2102 (1993).
- <sup>15</sup>V. Marchetti, J. Ghanbaja, P. Gérardin, and B. Loubinoux, *Holzforchung* **54**, 553 (2000).
- <sup>16</sup>S. Valencia, Ll. Balcells, B. Martínez, and J. Fontcuberta, *J. Appl. Phys.* **93**, 8059 (2003).
- <sup>17</sup>A. Biswas, M. Rajeswari, R. C. Srivastava, Y. H. Li, T. Venkatesan, R. L. Greene, and A. J. Millis, *Phys. Rev. B* **61**, 9665 (2000); A. Biswas, M. Rajeswari, R. C. Srivastava, T. Venkatesan, R. L. Greene, Q. Lu, A. L. de Lozane, and A. J. Millis, *ibid.* **63**, 184424 (2001).
- <sup>18</sup>X. J. Chen, H. U. Habermeyer, H. Zhang, G. Gu, M. Varela, J. Santamaria, and C. C. Almasan, *Phys. Rev. B* **72**, 104403 (2005).
- <sup>19</sup>Ll. Abad, B. Martínez, and Ll. Balcells, *Appl. Phys. Lett.* **87**, 212502 (2005).